LETTER • OPEN ACCESS

Influence of humidity on the binding of stone fragments via capillary bridges

To cite this article: B. N. J. Persson 2022 *EPL* **137** 46001

A Letters Journal Exploring the Frontiers of Physics

February 2022

EPL, **137** (2022) 46001
doi: 10.1209/0295-5075/ac5fcf

www.epljournal.org

Influence of humidity on the binding of stone fragments via capillary bridges

B. N. J. Persson[(a)]

PGI-1, FZ Jülich - Jülich, Germany and
MultiscaleConsulting - Wolfshovener str 2, 52418 Jülich, Germany

received 19 November 2021; accepted in final form 22 March 2022
published online 29 April 2022

Abstract – We study the humidity dependency of the adhesion (or pull-off) force between granite fragments and a silica glass plate. The particles bind to the glass plate via capillary bridges. The granite particles are produced by cracking a granite stone in a mortar and have self-affine fractal surface roughness. Theory shows that the surface roughness results in an interaction force between stone fragments and the glass plate which is independent of the size of the particles, in contrast to the linear size dependency expected for particles with smooth surfaces. We measure the adhesion force by depositing the granite particle powder, with particle sizes ranging from mm to μm (or less), on the glass plate. By turning the glass plate upside-down all particles with a gravitational force larger than the adhesion force will fall off the glass plate. By studying the size (and hence the mass) of biggest still attached particles we obtained the adhesion force, which is found to be in good agreement with the theory prediction.

Introduction. – Elastically stiff solid objects usually attract each other very weakly, and the force needed to separate two solid objects, *e.g.*, a glass bottle from a table, is usually so small that it cannot be detected without a very sensitive instrument. The fundamental reason for this is surface roughness, which results in a very small contact area [1–6]. In fact, in an ideal case, for perfectly smooth surfaces, the van der Waals interaction is quite strong, *e.g.*, it is possible to keep the weight of a car with the van der Waals interaction acting over a surface area $\sim 1\,\mathrm{cm}^2$ (see ref. [3]). However, in practice this is never observed due to surface roughness and non-uniform bond breaking at the interface. We have recently shown that for elastically stiff solid objects with large surface roughness, like stone fragments produced by cracking, the van der Waals interaction, which acts between all solids, results in a pull-off force below 1 nN, which is less than the typical force needed to break a single chemical bond.

The pull-off forces measured for small particles are usually larger than expected from the van der Waals interaction. This is due to the formation of capillary bridges, which form spontaneously in a humid atmosphere between contacting solids with a hydrophilic interface. An interface is hydrophilic if $\cos\theta_1 + \cos\theta_2 > 0$, where θ_1 and θ_2 are the fluid contact angles on the two solids. The influence of capillary bridges on the adhesion between small particles is well known from everyday experience: dry sand may exhibit liquid-like flow, like in a sandglass (hourglass), while wet sand particles can adhere, and as result one can build sand sculptures on the beach.

We have recently shown theoretically [7] that surface roughness results in an interaction force between stone fragments which is independent of the size of the particles, in contrast to the linear size dependency expected for particles with smooth surfaces. Here we study experimentally the dependency of the adhesion (or pull-off) force between granite fragments and a silica glass plate on the relative humidity. The granite particles are produced by cracking a granite stone in a mortar and have self-affine fractal surface roughness. We measured the adhesion force by depositing the powder of granite particles, with sizes ranging from mm to μm (or less), on the glass plate. By turning the glass plate upside-down all particles with a gravitational force larger than the adhesion force will fall off the glass plate. Studying the size (and hence the mass) of biggest still attached particles we obtained the adhesion

[(a)]E-mail: b.persson@fz-juelich.de (corresponding author)

Fig. 1: A particle in contact with a flat substrate in a humid atmosphere where a capillary bridge binds the solids together. The capillary bridge is in thermal (kinetic) equilibrium with the surrounding gas of water molecules. The solid objects are assumed perfectly rigid and they make contact in a single point.

force, which is found to be in good agreement with the theory prediction.

Theory. – We consider the model illustrated in fig. 1. A particle with a rough surface binds to a smooth surface in a humid atmosphere via a capillary bridge. The solid objects are assumed perfectly rigid and they make contact in a single point. The capillary bridge is in thermal (kinetic) equilibrium with the surrounding gas of water molecules determined by the relative humidity. We assume that the fluid (water) wets the solid surfaces so that $\theta_1 = \theta_2 = 0$. Following ref. [8], we put water at the interface in all surface regions where the surface separation $u(x, y)$ is below the critical separation $2t + h_c$, where t is the equilibrium thickness of the water film on the solid walls, and where h_c depends on the humidity and is given by the Kelvin equation [9–13].

The (macroscopic) Kelvin equation relates the equilibrium curvature of the liquid-vapor interface with the vapor pressure, as derived by equating the chemical potentials between two bulk phases:

$$\frac{1}{r_{\rm eff}} = \frac{k_{\rm B}T}{v\gamma} \ln \frac{P_{\rm S}}{P},$$

where $r_{\rm eff}$ is the mean radius of curvature such that $1/r_{\rm eff} = 1/r_1 + 1/r_2$ (where r_1 and r_2 are the two surface principal radii of curvatures) for the liquid meniscus. Here $k_{\rm B}$ is the Boltzmann constant, T is the temperature, γ the surface tension of water, $v = V/N \approx 29.7\,\text{Å}^3$ the volume of a water molecule in water and $P/P_{\rm S}$ the relative humidity ($P_{\rm S}$ and P are the saturated and actual water vapor pressure, respectively).

Both $2t$ and h_c depend on the humidity. For example, for the relative humidity $\sim 40\%$, for water $h_c \approx 2\,\text{nm}$ and (for amorphous silicone dioxide, silica) $2t \approx 2\,\text{nm}$ (see ref. [9]). The (negative) pressure in the capillary bridges is given by the Laplace pressure $p \approx -\gamma/r_c$, where $r_c = h_c/2$ is the radius of curvature of the capillary bridge (see fig. 1) at the vapor-fluid interface (here we have neglected a small corrections denoted the Tolman length arising from the dependency of the surface tension on the fluid curvature at the vapor-fluid interface) [10,14].

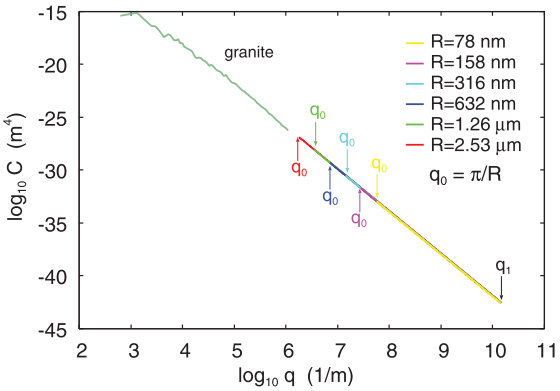

Fig. 2: The curved line is the measured power spectrum of the granite surface and the straight line the (extrapolated) power spectra used for the (granite) particles with the radius indicated in the figure. The small wave number (long wavelength) cut-off q_0 are indicated for each particle size while the large wave number (short wavelength) cut-off q_1 is the same in all cases. The straight line has the slope -4 corresponding to the Hurst exponent $H = 1$.

No two natural stone particles have the same surface roughness, and the adhesion force between two particles will depend on the particles used. To take this into account we have generated particles (with linear size $L = 2R$) with different random surface roughness but with the same surface roughness power spectrum. That is, we use different realizations of the particle surface roughness but with the same statistical properties. For each particle size we have generated 60 particles using a different set of random numbers. The surface roughness was generated as described in ref. [1] (appendix A) by adding plane waves with random phases $\phi_{\rm q}$ and with the amplitudes determined by the power spectrum,

$$h(x) = \sum_{\rm q} B_{\rm q} e^{i(q\cdot x + \phi_{\rm q})} \qquad (1)$$

where $B_{\rm q} = (2\pi/L)[C(\mathbf{q})]^{1/2}$. We assume isotropic roughness so $B_{\rm q}$ and $C(\mathbf{q})$ only depend on the magnitude of the wavevector $\mathbf{q}$.

We have used nominally spherical particles with 6 different radii, where the radius increases in steps of a factor of 2 from $R = 78\,\text{nm}$ to $R = 2.53\,\mu\text{m}$. The longest wavelength roughness which can occur on a particle with radius R is $\lambda \approx 2R$ so when producing the roughness on a particle we only include the part of the power spectrum between $q_0 < q < q_1$ where $q_0 = \pi/R$ and where q_1 is a short distance cut-off corresponding to atomic dimension (we use $q_1 = 1.4 \times 10^{10}\,\text{m}^{-1}$). This is illustrated in fig. 2 which shows the different short wave number cut-off q_0 used. We will refer to the particles with the power spectra shown in fig. 2 as granite particles because the power spectra used are linear extrapolation to larger wave number of the measured granite power spectrum.

We note that the theory we use is only valid as long as the height h_c of the water capillary bridge is small

compared to the radius R of the particle [15]. Here we apply the theory only to cases where all the water in the capillary bridge is located within a circular region $r < 0.5R$ in the xy plane, where $r = 0$ is the point where the sphere (without surface roughness) touches the flat surface. This implies that $h_c < r^2/(2R) = R/8$. For a given humidity (and hence given h_c) this will determine the minimum particle radius for which we apply the theory.

In the theory we have neglected elastic deformations of the solids. For elastically stiff solids, *e.g.*, granite and silica glass, elastic deformations have a very small influence on the pull-off force because the maximum of the tensile force occurs close to the point where the solids make contact in a single point. Thus, during separation, starting from the equilibrium state (no external force) where the attractive force balances the repulsive force occurring in the central part of the contact, the elastic repulsion is gradually reduced and close to the point where the repulsive force vanishes the tensile force will be maximal. This is well known for the contact between two perfectly smooth and elastically stiff spheres where the pull-off force is maximal exactly at the point where the two spheres touch in a single point. This follows by comparing the results of Bradley [16] and Derjaguin [17] for rigid spheres, with the theory of Derjaguin-Muller-Toporov (DMT) [18] for elastic spheres: in both cases the pull-off force is given by $2\pi w R_{\rm eff}$ where w is the work of adhesion ($w = 2\gamma$ in the present case), *i.e.*, the elastic deformations in the equilibrium state has no influence on the pull-off force. We do note, however, if the contact stress gets big enough during the approach-retraction cycle it can result in plastic deformations of the asperities (or the bulk below the asperities), and this could strongly increase the pull-off force as it would effectively smooth the surfaces. This effect was proposed in ref. [2] for a PMMA sphere squeezed against silicon wafers, and observed in two recent studies [13,19].

The situation for elastically soft solids is completely different than for elastically stiff solids. Thus for soft solids elastic deformations will in general have a huge influence on the pull-off force [20–25]. This may at first appear unexpected since the famous Johnson-Kendall-Roberts (JKR) [26] theory predicts a pull-off force $(3/2)\pi w R_{\rm eff}$ which is independent of the elastic modulus, but this result holds only for a particular geometry (for parabolic particles with perfectly smooth surfaces) [27] and is not valid in more general situations, *e.g.*, when the spheres have surface roughness.

Numerical results. – Since no two particles will have the same surface roughness, the pull-off force will depend on the particular particle studied. To illustrate this, fig. 3 shows the cumulative probability for the pull-off force assuming capillary (relative humidity $P/P_s = 0.4$) and VDW interaction (dry contact). The probability distributions are obtained from 60 simulations for each particle radius (for 6 different particles radii). The 60 simulations use 60 different realizations of the particle surfaces topography

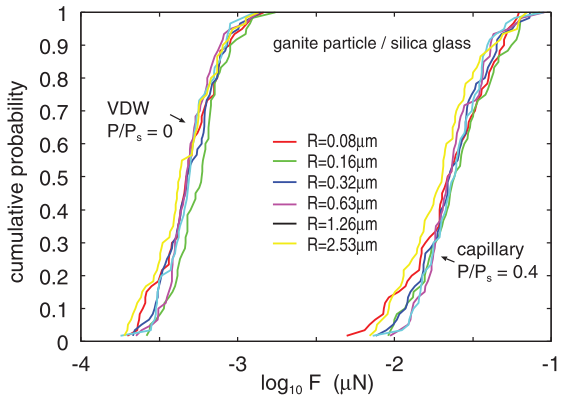

Fig. 3: The cumulative probability for the pull-off force assuming capillary (relative humidity $P/P_s = 0.4$) and VDW interaction (dry contact). The probability distributions are obtained from 60 simulations for each particle radius (for 6 different particles radii). The 60 simulations use 60 different realizations of the particle surfaces topography but with the same power spectra.

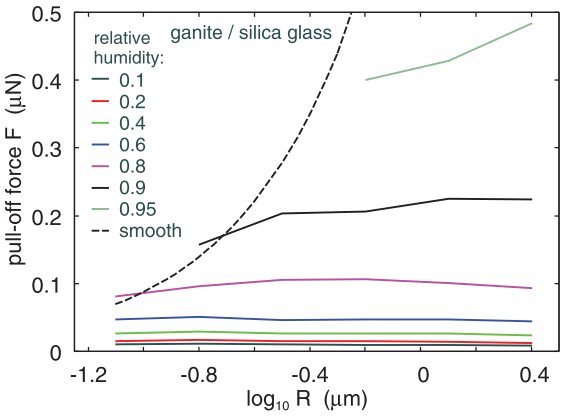

Fig. 4: The calculated dependency of the pull-off force on the relative humidity for granite particles in contact with a borosilica glass plate. The pull-off force is given as a function of the particle radius for the relative humidities $P/P_S = 0.1$, 0.2, 0.4, 0.6, 0.8, 0.9 and 0.95. The dashed line shows the results for a spherical granite particle with perfectly smooth surface.

but with the same power spectra. The VDW interaction is for dry surfaces ($P/P_s = 0$) and was treated as described in ref. [7]. The VDW interaction gives a pull-off force nearly 100 times smaller than for the capillary interaction and in a humid atmosphere it will be even smaller and we will neglect it in what follows. The average pull-off force due to capillary bridges at the relative humidity $P/P_s = 0.4$ is $F \approx 0.027\,\mu$N and the standard deviation $\approx 0.015\,\mu$N.

Figure 4 shows the calculated dependency of the pull-off force on the relative humidity for granite particles in contact with a borosilica glass plate. The pull-off force is given as a function of the particle radius for the relative humidity's $P/P_S = 0.1$, 0.2, 0.4, 0.6, 0.8, 0.9 and 0.95. The dashed line shows the results for a spherical granite

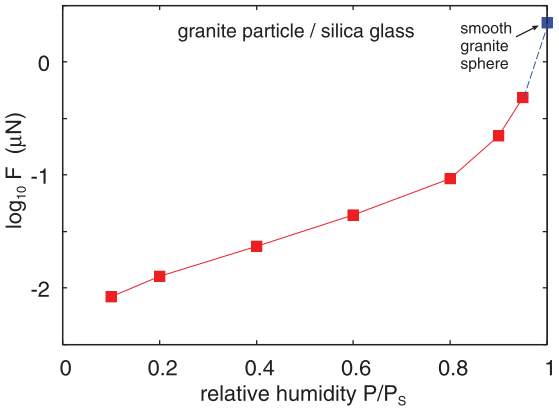

Fig. 5: The calculated dependency of the logarithm of the pull-off force on the relative humidity for a granite particle with the radius $R = 2.529\,\mu$m in contact with a borosilica glass plate. The blue square for the relative humidities $P/P_S = 1$ is for a smooth spherical granite particle.

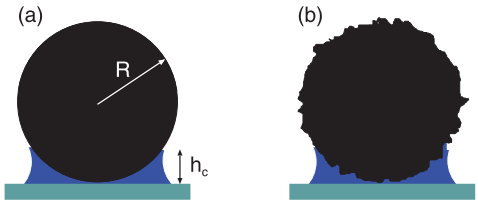

Fig. 6: When the height h_c of the capillary bridge becomes comparable with (but less than) the radius R of the particle, then the region occupied by the fluid in the capillary bridge will be similar for the smooth particle in (a) as for the rough particle in (b).

particle with perfectly smooth surface. Note that for a given humidity the height of the capillary bridge is given. The theory we use is only valid when the particle radius R is much larger than the height h_c of the capillary bridge (see the second section). For this reason the theory curves for the two highest humidities in fig. 4 do not start at the smallest particle radius used in the simulations, but for a larger particle radius ($R > 8h_c$).

Figure 5 shows the dependency of the pull-off force on the relative humidity for a granite particle with the radius $R = 2.529\,\mu$m in contact with a borosilica glass plate obtained from the results in fig. 4. Figure 5 shows the same but with the logarithm of the pull-off force. The blue square for the relative humidity $P/P_S = 1$ is for a smooth spherical granite particle with the same radius $R = 2.529\,\mu$m as for the rough particles. Note that the calculated results for rough particles extrapolate smoothly towards the result for smooth particles as the humidity approaches 1 (see dashed line in fig. 5). This is expected because for large humidity the region filled with water will be similar in both cases (see fig. 6).

Experimental. – We have measured the humidity dependency of the adhesion (or pull-off) force between

Fig. 7: Experimental set-up. Granite powder is produced in a mortar and deposited on a glass plate located in a closed box. The glass plate is cleaned with soap water, acetone and isopropanol. The humidity in the closed box is changed by including in the box a cup of water or humidity absorbing salt. The glass plate with granite powder is kept in the box for 24 hours to obtain thermal (kinetic) equilibrium between the water molecules at the interface and in the gas phase.

granite fragments and a silica glass plate, for the relative humidities $P/P_s = 0.18$, 0.6, 0.9 and 0.99, using a hygrometer with the accuracy ± 0.02. The particles bind to the glass plate via capillary bridges. As shown in ref. [7] the contribution to the adhesion force from the van der Waals interaction is negligible in this humidity range so the main contribution to the pull-off force is assumed to originate from capillary bridges.

The granite particles are produced by cracking a granite stone in a mortar (see fig. 7), and they have self-affine fractal surface roughness, with the Hurst exponent $H \approx 1$, at least in the wave number region probed by our stylus instrument (see curved line in fig. 2). We measure the adhesion force by depositing on the glass plate the powder of granite particles, with sizes ranging from mm to μm (or less). The glass plate is kept in a closed box with fixed humidity for 24 hours to reach thermal (kinetic) equilibrium between water at the interface and in the gas phase. By turning the glass plate upside-down all particles with a gravitational force larger than the adhesion force will fall off the glass plate. Since the pull-off force is (nearly) independent of the size of the particles, by studying the size (and hence the mass) of the biggest still attached particles we obtain the adhesion force at any given humidity.

Using an optical microscope we have studied the particles remaining on the glass plate after turning it upside-down. Turning the plate upside-down results in the detachment of a large number of particles. Of the remaining (huge number of) particles bound to the glass plate it is possible to detect by the naked eye the biggest particles, the size of which we measured using the optical microscope. We will refer to the ~ 10 biggest particles, which all have similar size, as the big particles. Within the xy plane (parallel to the glass plate) we denote the

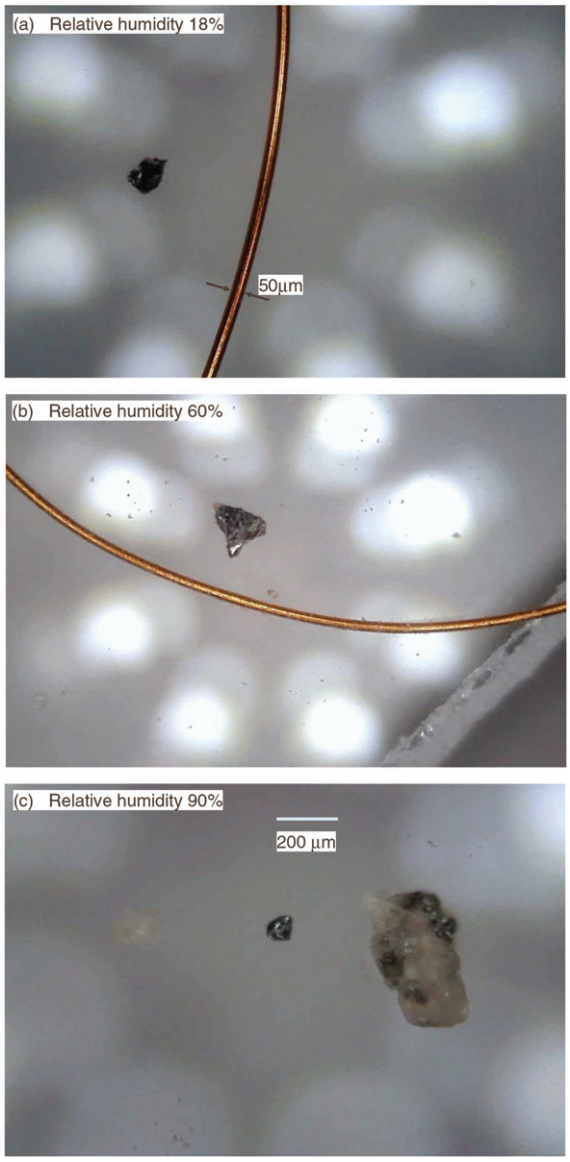

Fig. 8: Pictures of big particles adhering to a glass plate at the relative humidity (a) 18%, (b) 60% and (c) 90%. The copper wire in (a) and (b) has the diameter 50 μm. The particle in (a) has the length and width 150 and 130 μm, respectively, and in (c) the big particle has the length and width 600 and 300 μm, respectively.

longest length of a particle by a_x and the length in the orthogonal direction by a_y. The length a_z of the particle in the direction orthogonal to the glass plate could not be measured using our optical microscope. However, studies have shown that particles produced by cracking stones (with isotropic statistical properties) have in general similar length in all directions [28,29], were here we assume (quite arbitrarily) $a_z \approx (a_x a_y)^{1/2}$. We assume the shape of the particles can be approximated by ellipsoids so that the volume $V = (\pi/6)a_x a_y a_z \approx (\pi/6)(a_x a_y)^{3/2}$. The gravitational force acting on a particle when the glass plate is in the turned upside-down state is $F_{\rm G} = Mg = \rho V g$ where $\rho \approx 2.7\,{\rm g/cm^3}$ is the granite mass density and

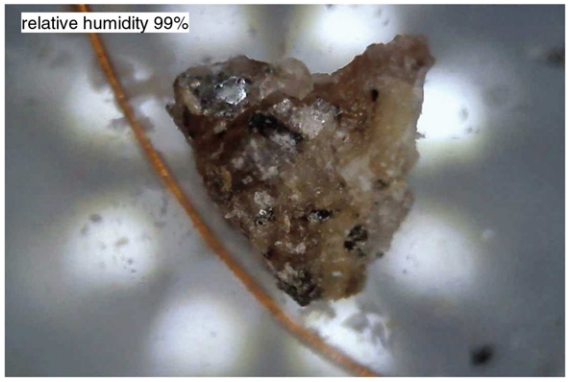

Fig. 9: At the relative humidity 99% no particle detached as the glass plate was turned upside-down. The largest attached particles have a diameter of order 1 mm.

$g \approx 9.81\,{\rm m/s^2}$ the gravitational acceleration. For the biggest particles $F_{\rm G} = F_{\rm ad}$. If we measure V in mm^3 we get $F_{\rm G} = [26.5\,\mu{\rm N}] \times V$.

Figure 8 shows pictures of big particles adhering to a glass plate at the relative humidity (a) 18%, (b) 60% and (c) 90%. The copper wire in (a) and (b) has the diameter 50 μm. The particle in (a) has the length and width 150 and 130 μm, respectively, and in (c) the big particle has the length and width 600 and 300 μm, respectively. At the relative humidity 99% no particle detached from the glass plate as it was turned upside-down. Figure 9 shows a big particle (with a diameter of order 1 mm) for this case. In this case we can only give a lower bound on the adhesion force which is $F \approx 50\,\mu$N. For a smooth sphere with the diameter $D = 1.2$ mm theory predicts the pull-off force (independent of the humidity) $F = 2\pi\gamma D \approx 500\,\mu$N.

Comparison of theory with experiments. – Figure 10 shows the calculated (red squares) and measured (green stars) dependency of the logarithm of the pull-off force on the relative humidity for granite particles in contact with a borosilica glass plate. The measured pull-off force is divided by a factor of 3 to take into account three (assumed) contact points. In the theory the particle radius $R = 2.529\,\mu$m, while in the experiment the typical radii of the granite particles are 450 μm at 90% relative humidity and 140 μm at 18% relative humidity. The blue square is the theory prediction for the relative humidity $P/P_{\rm S} = 1$ for a smooth spherical granite particle with the radius $R = 2.529\,\mu$m.

In the experiments the effective diameter $D = (abc)^{1/3}$ of the biggest particles is about 140 μm for 18% relative humidity and 450 μm for 90% relative humidity (see fig. 8). These particle diameters are much larger than that used in the theory calculations which was $D = 2R \approx 5\,\mu$m. If the particles were perfectly smooth spheres the pull-off force would scale linearly with D, and would hence be ≈ 100 times bigger in the experiment than in the theory. However, fig. 10 shows that within the statistical noise there is good agreement between theory and experiments. This

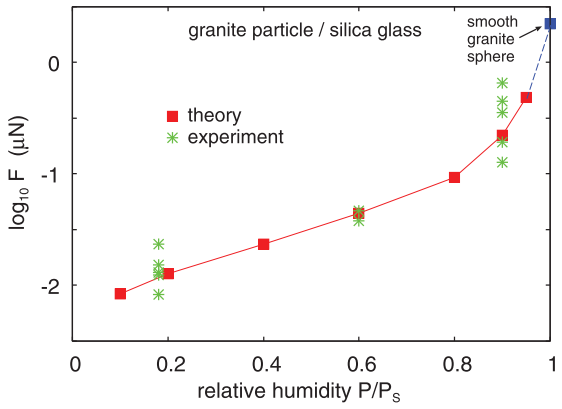

Fig. 10: The calculated (red squares) and measured (green stars) dependency of the logarithm of the pull-off force on the relative humidity for granite particles in contact with a borosilica glass plate. The measured pull-off force is divided by a factor of 3 to take into account three (assumed) contact points. In the theory the particle radius $R = 2.529\,\mu$m while the typical diameter of the granite particles are $400\,\mu$m at 90% relative humidity and $140\,\mu$m at 18% relative humidity. The blue square is the theory prediction for the relative humidity $P/P_S = 1$ for a smooth spherical granite particle with the radius $R = 2.529\,\mu$m.

shows that for particles with (high enough) roughness, the pull-off force is independent of the particle diameter, as indeed predicted by the theory.

Discussion. – There are several assumptions made above which I would like to briefly address.

a) I have assumed that there are three contact points between the granite particles and the substrate glass plate and that the contact breaks simultaneously so that the pull-off force is three times the pull-off force to break one contact point. This would probably be the case for a very symmetric particle but may not hold accurately in general.

b) When calculating the volume of a particle we assumed it to be ellipsoidal with the length a_x, a_y and a_z in the three axial directions so that $V = (\pi/6)a_x a_y a_z$. We assumed also that the length of the particle orthogonal to the glass plate is $a_z = (a_x a_y)^{1/2}$ so that $V = (\pi/6)(a_x a_y)^{3/2}$. However, one may argue that it is more likely that the length a_z orthogonal to the glass plate is the shortest as this would minimize the potential energy and give a more stable binding configuration. In ref. [29] it was found that if $a_x > a_y > a_z$ then the volume $V \approx (\pi/6)k(a_x a_y)^{3/2}$ where $k \approx 0.3$. The study in ref. [29] also gives information about the fluctuations in the particle volume given the area number $a_x a_y$. The particle fragments analyzed in ref. [29] were produced in high impact velocity collisions (5–6 km/s) so different from our granite fragments produced in a mortar. Using this expression we would obtain a particle volume a factor of ≈ 0.3 smaller than with the procedure used above.

c) We have observed that during the turn-around of the glass plate with the granite powder some particles slide off the plate before the plate is turned around. This could effectively reduce the observed pull-off force and would partly compensate for the effect described in (b).

Summary. – We have presented experimental results for the pull-off force between granite stone fragments and a silica glass plate for different humidities. The experimental results are in good agreement with the theory predictions. The experiments involves particles typically 100 times bigger than in the theory calculations. If the particles were spheres with perfectly smooth surfaces theory would predict that the pull-off force is proportional to the particle diameter, but for particles with big enough roughness the theory predicts that the pull-off force is independent of the size of the particles, which is supported by our experimental results.

The results obtained in this study, and in [7], are fundamental for many applications, *e.g.*, the rheology of granular materials [30], or the adhesion of hard dust particles (such as mineral particles in dust storms) to different surfaces [31]. Other examples are the adhesion and removal of particles from wafer for electronic applications [32] or from spacecraft [33]. Capillary bridges are also involved in insect adhesion pads but in this case it is likely necessary to include elastic deformations of the adhesive system [34–36].

* * *

We thank Jens Biele (German Aerospace Center) for comments on the manuscript.

REFERENCES

[1] Persson B. N. J., Albohr O., Tartaglino U., Volokitin A. I. and Tosatti E., *J. Phys.: Condens. Matter*, **17** (2004) R1.
[2] Persson B. N. J., *Surf. Sci. Rep.*, **61** (2006) 201.
[3] Ciavarella M., Joe J., Papangelo A. and Barber J. R., *J. R. Soc. Interface*, **16** (2019) 20180738.
[4] Vakis Antonis I., Yastrebov Vladislav A., Scheibert Julien, Nicola Lucia, Dini Daniele, Minfray Clotilde, Almqvist Andreas, Paggi Marco, Lee Seunghwan, Limbert Georges, Molinari Jean-Francois, Anciaux Guillaume, Aghababaei Ramin, Echeverri Restrepo S., Papangelo Antonio, Cammarata Antonio, Nicolini Paolo, Putignano Carmine, Carbone Giuseppe, Stupkiewicz Stanislaw, Lengiewicz Jakub, Costagliola Gianluca, Bosia Federico, Guarino Roberto, Pugno Nicola M., Müser Martin H. and Ciavarella Michele, *Tribol. Int.*, **125** (2018) 169.
[5] Rabinovich Y. I., Adler J. J., Ata A., Singh R. K. and Moudgil B. M., *J. Colloid Interface Sci.*, **232** (2000) 10.

[6] Wang A. and Müser M. H., *Is there more than one stickiness criterion?*, submitted to *Friction* (2022).
[7] Persson B. N. J. and Biele J., *Tribol. Lett.*, **70** (2022) 34.
[8] Persson B. N. J., *J. Phys.: Condens. Matter*, **20** (2008) 315007.
[9] Asay D. B. and Kim S. H., *J. Phys. Chem. B*, **109** (2005) 16760.
[10] Kim S., Kim D., Kim J., An S. and Jhe W., *Phys. Rev. X*, **8** (2018) 041046.
[11] van Zwol P. J., Palasantzas G. and De Hosson J. T. M., *Appl. Phys. Lett.*, **91** (2007) 101905.
[12] Soylemez E. and de Boer M. P., *Langmuir*, **30** (2014) 11625.
[13] Hsia F. C., Franklin S., Audebert P., Brouwer A. M., Bonn D. and Weber B., *Phys. Rev. Res.*, **3** (2021) 043204.
[14] Israelachvili J., *Intermolecular and Surface Forces* (Academic Press) 2011.
[15] Chen L. and Qian L., *Friction*, **9** (2021) 1.
[16] Bradley R. S., *London Edinburgh Dublin Philos. Mag. J. Sci.*, **13** (1932) 853.
[17] Derjaguin B. V., *Kolloid-Z.*, **69** (1934) 155.
[18] Derjaguin B. V., Muller V. M., Toporov Y. P., *J. Colloid Interface Sci.*, **53** (1975) 314.
[19] Thimons L. A., Gujrati A., Sanner A., Pastewka L. and Jacobs T. D. B., *Exp. Mech.*, **61** (2021) 1109.
[20] Tiwari A., Wang J. and Persson B. N. J., *Phys. Rev. E*, **102** (2020) 042803.
[21] Tiwari A., Dorogin L., Bennett A. I., Schulze K. D., Sawyer W. G., Tahir M. and Persson B. N. J., *Soft Matter*, **13** (2017) 3602.
[22] Pastewka L. and Robbins M. O., *Proc. Natl. Acad. Sci. U.S.A.*, **111** (2014) 3298.
[23] Fuller K. N. G. and Tabor D., *Proc. R. Soc. London Ser. A*, **345** (1975) 327.
[24] Ciavarella M., *Tribol. Int.*, **146** (2020) 106031.
[25] Müser M. H., *Tribol. Int.*, **100** (2016) 41.
[26] Johnson K. L., Kendall K. and Roberts A. D., *Proc. R. Soc. London A: Math. Phys. Sci.*, **324** (1971) 301.
[27] Barthel E., *J. Phys. D: Appl. Phys.*, **41** (2008) 163001.
[28] Domokos G., Kun F., Sipos A. A. and Szabo T., *Sci. Rep.*, **5** (2015) 9147.
[29] Michikami T. and Hagermann A., *Icarus*, **357** (2021) 114282.
[30] Mandala S., Nicolasa M. and Pouliquen O., *Proc. Natl. Acad. Sci. U.S.A.*, **117** (2020) 8366.
[31] Adukwu J. E., Yilbas B. S., Jalilov A. S., Al-Qahtani H., Yaqubu M., Abubakar A. A. and Khaled M., *Sci. Rep.*, **10** (2020) 13812.
[32] Menon V. B., Michaels L. D., Donovan R. P., Debler V. L. and Ranade M. B., *Particle removal from semiconductor wafers using cleaning solvents*, in *Particles in Gases and Liquids 1*, edited by Mittal K. L. (Springer, Boston, Mass.) 1989.
[33] Hartzell C. M., Farrell W. and Marshall J., *Adv. Space Res.*, **62** (2018) 2213.
[34] Langer M. G., Ruppersberg J. P. and Gorb S. N., *Proc. R. Soc. London B*, **271** (2004) 2209.
[35] Hosoda N. and Gorb S. N., *Proc. R. Soc. B*, **279** (2012) 4236.
[36] Kovalev A. E., Filippov A. E. and Gorb S. N., *J. R. Soc. Interface*, **10** (2013) 1.